

Complementary Patterns of Gene Expression by Human Oligodendrocyte Progenitors and Their Environment Predict Determinants of Progenitor Maintenance and Differentiation

Fraser J. Sim, PhD,¹ Jennifer K. Lang, BS,¹ Ben Waldau, MD,¹ Neeta S. Roy, PhD,² Theodore E. Schwartz, MD,³ Webster H. Pilcher, MD, PhD,⁴ Karen J. Chandross, PhD,⁵ Sridaran Natesan, PhD,⁶ Jean E. Merrill, PhD,⁵ and Steven A. Goldman, MD, PhD^{1,2}

Objective: Glial progenitor cells are abundant in adult human white matter. This study was designed to identify signaling pathways regulating their self-renewal and fate.

Methods: We compared the transcriptional profiles of freshly sorted adult human white matter progenitor cells (WMPCs), purified by A2B5-based immunomagnetic sorting, with those of the white matter from which they derived.

Results: We identified 132 genes differentially expressed by WMPCs; these included principal components of five receptor-defined signaling pathways, represented by platelet derived growth factor receptor alpha (PDGFRA) and type 3 fibroblast growth factor receptor (FGFR3), receptor tyrosine phosphatase- β/ζ (RTPZ), notch, and syndecan3. WMPCs also differentially expressed the bone morphogenetic protein 4 (BMP4) inhibitors neuralin and BAMBI (BMP and activin membrane-bound inhibitor), suggesting tonic defense against BMP signaling. Differential overexpression of RTPZ was accompanied by that of its modulators pleiotrophin, NrCAM, tenascin, and the chondroitin sulfate proteoglycans, suggesting the importance of RTPZ signaling to WMPCs. When exposed to the RTPZ inhibitor bpV(phen), or lentiviral-shRNAi against RTPZ, WMPCs differentiated as oligodendrocytes. Conversely, when neuralin and BAMBI were antagonized by BMP4, astrocytic differentiation was induced, which was reversible by noggin.

Interpretation: The RTPZ and BMP pathways regulate the self-maintenance of adult human WMPCs, and can be modulated to induce their oligodendrocytic or astrocytic differentiation. As such, they provide targets by which to productively mobilize resident progenitor cells of the adult human brain.

Ann Neurol 2006;59:763–779

A population of nominally glial progenitor cells resides in the parenchyma of the adult human subcortical white matter. These cells may be defined by A2B5 immunoreactivity and by their expression of fluorescent reporters placed under the control of the CNP2 promoter.^{1,2} The cells typically act as oligodendrocyte progenitors, yielding myelinogenic oligodendrocytes on transplantation.³ However, when removed from the tissue environment, they behave as multipotential and neurogenic progenitor cells.² This observation suggested that the local tissue environment regulates both the self-renewal and phenotype of parenchymal glial progenitors, such that the latter actually represents a pool of multipotential progenitors, whose fate is tonically restricted by their local tissue environment. As a

result, the environmental cues presented to these cells, and their responsiveness to these signals, may determine not only their mitotic turnover, but also their undifferentiated self-renewal and postmitotic lineage choices. Yet no studies to date have specifically examined the environment of the adult human white matter from the standpoint of the steady-state cues and cell-specific responsiveness of resident progenitor cells.

To identify genes that regulate the turnover and fate decisions of adult glial progenitor cells in vivo, we used U95Av2 Affymetrix microarrays (Affymetrix, Santa Clara, CA) to analyze the transcriptional profile of A2B5⁺ white matter progenitor cells (WMPCs), sorted from human white matter samples derived from surgically resected adult temporal lobe. The profile of each

From the ¹Department of Neurology, University of Rochester Medical Center, Rochester; Departments of ²Neurology and ³Neurosurgery, Cornell University Medical Center, New York; ⁴Department of Neurosurgery, University of Rochester Medical Center, Rochester, NY; ⁵Aventis Pharmaceuticals, Bridgewater, NJ; and ⁶Cambridge Genomics Center, Aventis, Cambridge, MA.

Received Aug 23, 2005, and in revised form Dec 9. Accepted for publication Dec 16, 2005.

This article includes supplementary materials available via the Internet at <http://www.interscience.wiley.com/jpages/0364-5134/suppmat>

Published online Apr 24, 2006 in Wiley InterScience (www.interscience.wiley.com). DOI: 10.1002/ana.20812

Address correspondence to Dr Goldman, Department of Neurology, University of Rochester Medical Center, 601 Elmwood Road, Box 645, Rochester, NY 14642. E-mail: steven_goldman@urmc.rochester.edu

sorted cell population was then normalized against that of the unsorted dissociate from which it was derived, to identify WMPC-enriched transcripts that were otherwise underrepresented in the white matter. By this strategy, we identified several unexpected ligands and receptors and their attendant signaling pathways, which appear to uniquely characterize the interaction of oligodendrocyte progenitor cells with the ambient white matter in which they reside. From these data, we then assessed the functional importance of two of these pathways, and confirmed that their modulation permitted us to directly manipulate the fate of initially uncommitted WMPCs.

Materials and Methods

Cell and Tissue Samples

Adult human subcortical white matter was obtained from temporal lobe tissue removed from 18 patients at craniotomy, principally for medication-refractory epilepsy (age, 17–56 years; 12 male and 6 female patients). Samples were obtained from patients who consented to tissue use under protocols approved by the New York Hospital-Cornell, Columbia Presbyterian Hospital, and University of Rochester-Strong Memorial Hospital Institutional Review Boards. The tissues were prepared and WMPCs freshly isolated as described previously.² In brief, samples were minced into PIPES solution (in mM: 120 NaCl, 5 KCl, 25 glucose, and 20 PIPES), then digested in papain-PIPPES (11.4U/ml papain; Worthington, Freehold, NJ) and DNase I (10U/ml; Sigma, St. Louis, MO), on a shaker for 1.5 hours at 37°C. The cells were collected by centrifugation at 200g in an International Equipment Company (IEC) Centra-4B centrifuge, resuspended in Dulbecco's minimum essential medium (DMEM)/F-12/N1 with +DNase I (10U/ml), and incubated for 30 minutes at 37°C. The samples were again spun, and their pellets recovered in 2ml of DMEM/F-12/N1. They were then dissociated by sequentially triturating for 20, 10, and 5 times, respectively, through 3 glass Pasteur pipettes fire polished to decreasing bore diameters. The cells were passed through a 40µm mesh into DMEM/F-12/N1, with 10% plasma-derived fetal bovine serum (PD-FBS; Cocalico Biologicals, Reamstown, PA) to stop the enzymatic dissociation. The cells were then suspended in DMEM/F12/N1 and incubated in A2B5 antibody containing supernatant (clone 105; American Type Culture Collection, Manassas, VA) for 30 to 45 minutes at 4°C on a shaker. The cells were washed three times with phosphate-buffered saline containing 0.5% bovine serum albumin and 2mM EDTA, then incubated with 1:4 diluted microbead-tagged rat anti-mouse IgM antibody (magnetic-activated cell sorting [MACS]; Miltenyi Biotech, Auburn, CA) for 30 minutes at 4°C on a shaker. The A2B5⁺ cells were washed, resuspended, and separated using positive selection columns, type MS+/RS+ or LS+/VS+ (MACS; Miltenyi Biotech). The number of viable cells was determined by calcein (Molecular Probes, Eugene, OR).

RNA Extraction and Affymetrix GeneChip Protocol

Four samples were used for genomic analysis, microarray, and quantitative polymerase chain reaction (qPCR) valida-

tion. Immediately after sorting, RNA was extracted with Trizol (Invitrogen, La Jolla, CA) and purified using RNeasy (Qiagen, Chatsworth, CA), both according to manufacturers' specifications. All four samples were used for qPCR validation. Three samples were profiled using Affymetrix microarrays, 100ng of total RNA was amplified using Affymetrix's small sample protocol (GeneChip Eukaryotic Small Sample Target Labeling Technical Note), and 15µg of complementary RNA was used on each U95Av2 GeneChip.

Analysis of GeneChip Expression Data

DATA ANALYSIS. Image files were processed using MAS5.0 to produce CHP files. Images were masked to remove streaks or smears, and no scaling of data was performed during analysis. Data were then imported into GeneSpring (6.1; Silicon Genetics, Palo Alto, CA), and per chip normalization performed, using the 50th percentile of all measurements in that sample. Calculation of gene expression ratios was then performed by comparing the expression pattern of each A2B5-sorted sample with that of the unsorted population from which it had been extracted. This comparison effectively normalized sample-to-sample variation. The arithmetic mean ratio of A2B5 sorted-to-unsorted was then calculated from three separate patients. An estimate of error was generated using the Rocke-Lorenzato global error model,⁴ which takes into account the variability in the expression level of individual genes, compared with that of the entire data set. As a result, lower and more variably expressed genes are given larger error values, and are thus less likely to be deemed significant using our statistical criteria. Transcripts deemed significantly enriched or depleted in the sorted cell pool were selected using a two-way paired *t* test utilizing a Benjamini and Hochberg false discovery rate of 10%.⁵

ANNOTATION OF PROBE SETS. Qualifying probe sets for each gene on the Affymetrix Human U95Av2 chip were identified using annotations available from NetAffx (www.affymetrix.com/analysis) and Ensembl (www.ensembl.org/human). Probe sets with conflicting annotations were verified by BLAST analysis of probe target sequence to the human genome. This process excluded misannotated probe sets. Annotation and further data analysis was then performed within an in-house Microsoft Access database.

REAL-TIME POLYMERASE CHAIN REACTION. Our choice of genes validated by quantitative reverse transcriptase PCR was designed to efficiently test the model that we generated based on array data alone (see Fig 4). Primers and probes were either designed using Primer express (Applied Biosystems, Foster City, CA), or obtained as Assays-on-Demand from Applied Biosystems (www.allgenes.com). For each sample, four separate reverse transcription reactions of 25ng total RNA were performed as per the manufacturer's protocol, and the resulting complementary DNA diluted to 100pg/µl. Four separate real-time PCRs with 500pg per reaction, in addition to no-RT control reactions, were performed to rule out RNA-independent product amplification. For *TaqMan* real-time PCR, we used 900nM forward and reverse primers, and 250nM FAM-labeled MGB probes. For SYBR Green real-time PCR, we used 300nM forward and reverse primers.

Human 18S RNA was used as an endogenous control, as described by the manufacturer (ABI, Foster City, CA). The relative abundance of transcript expression was calculated following normalization of the C_t value to the matched unsorted white matter dissociate control, and the final expression ratio was then normalized to the endogenous control. The mean, standard error, and significance testing of the individual samples were calculated by first performing a log transformation on the ratio data; the values presented are the anti-log of these values. Significance was tested using a two-way, one-sample t test against a null ratio of 1 ($n = 4$).

Lentiviral Receptor Tyrosine Phosphatase- β/ζ RNAi Production and Validation

We constructed an RNAi knock-down vector specific for the long receptor isoform of receptor tyrosine phosphatase- β (RTPZ). shRNAi oligonucleotides were designed against exon 7 of RTPZ using the siRNA selection program⁶ and ligated into the lentiviral backbone pLL3.7 (ATCC).⁷ Lentiviral RTPZ RNAi was produced by quadruple transfection of the pLL3.7 lentiviral plasmid with helper plasmids pLP/VSVG, pLP1, and pLP2 (Invitrogen) into 293T cells with FuGene (Roche Applied Science, Indianapolis, IN). Viral supernatants were collected at 48 and 72 hours and concentrated by ultrafiltration using Centricon Plus-80 (100,000kDa) filters (Millipore, Bedford, MA), yielding a titer of approximately 10^8 plaque-forming U/ml.

Knock-down efficiency was validated in the glioblastoma cell line, U373-MG, which expresses high levels of RTPZ.⁸ Following lentiviral infection, GFP⁺ cells were fluorescence-activated cell sorted to purity, and both RNA and protein extracted. Real-time reverse transcriptase PCR using long isoform specific primers (see Supplementary Table 3) showed U373-MG RTPZ shRNAi/GFP⁺ cells to have more than 90% knock-down of the RTPZ messenger RNA (mRNA) compared with a scrambled shRNAi control virus or uninfected controls (see the Supplementary Fig). Western analysis using RTPZ-specific primary antibody (BD Pharmingen, San Diego, CA) showed that the expression of a 250kDa band in control U373-MG cell was completely abolished in RTPZ shRNAi/GFP⁺ cells.

In Vitro Challenge

Following dissociation and A2B5⁺-based MACS isolation, WMPCs were distributed onto 12-well plates coated with poly-L-ornithine and fibronectin at 5×10^4 cells/ml in DMEM/F12/N1 supplemented with 10ng/ml basic fibroblast growth factor (bFGF; Sigma), 10ng/ml PDGF-AA (Sigma), and 2ng/ml NT3 (R&D Systems, Minneapolis, MN). Cells were further exposed to inhibitor treatment, lentiviral RNAi, and factor addition to assess WMPC responses. Potassium bisperoxo(1,10-phenanthroline)oxovanadate (V) (referred to hereafter as bpV(phen); Calbiochem, San Diego, CA) was used as a potent receptor tyrosine phosphatase inhibitor. Stock solutions of 1mM bpV(phen) were prepared before each use. Cells were exposed to concentrations of 0, 1, 5, 10, and 25ng/ml of bpV(phen) immediately on plating, and every 2 days thereafter for 7 days in vitro. Alternatively, WMPCs were infected at a multiplicity of infection (MOI) of 50 with the RTPZ RNAi lentivirus in the presence of polybrene (8 μ g/ml)

for a total of 12 hours. WMPCs challenged with the addition of bone morphogenetic proteins (BMPs) were exposed to dosages of 0, 5, and 50ng/ml of BMP2, BMP4, and BMP7 (R&D Systems) for 4, 7, and 14 days in vitro. In addition, cells were both simultaneously and independently treated with 0, 20, and 100ng/ml of the BMP antagonist, noggin (Pepro-Tech, Rocky Hill, NJ) for 4, 7, and 14 days in vitro. To assess effect of treatment on WMPC proliferation, we pulsed cultures with 10 μ g/ml bromodeoxyuridine (BrdU) for 24 hours immediately prior to fixation.

Immunocytochemistry

After 7 to 14 days in vitro, cells were immunolabeled live for either A2B5 or O4 as described previously.¹ In brief, O4 supernatant (R. Bansal and S. Pfeiffer, University of Connecticut Health Center, Farmington, CT) was used at a dilution of 1:100 and monoclonal antibody A2B5 supernatant (clone 105, ATCC) was used in a 1:1 ratio with DMEM/F12/N, both for 40 minutes at 4°C. Secondary antibody, Texas Red-conjugated goat anti-mouse IgM was used at a dilution of 1:50 for 30 minutes. For multiple antigen labeling, O4 and A2B5 were localized on live cells that were then fixed with 4% paraformaldehyde and immunostained for glial fibrillary acidic protein (GFAP) and BrdU. Rabbit anti-GFAP antibody (Chemicon) was used at a dilution of 1:1,000. Rat anti-BrdU antibody (Oxford Biotechnology, Kidlington, UK) was used at a dilution of 1:200. Secondary antibodies, Alexa 594- and 647-conjugated goat-anti rabbit and rat antibodies, respectively, were used at a dilution of 1:400. Fixed cultures were then counterstained with DAPI (10ng/ml; Molecular Probes). The number of A2B5⁺GFAP⁻, A2B5⁺GFAP⁺, GFAP⁺A2B5⁻, and O4⁺ stained and unstained cells were counted in 10 randomly chosen fields at each dosage level, from two replicate samples at each dose for each patient sample. Statistical significance was assessed by one-way repeated-measures analysis of variance (ANOVA) followed by Bonferroni multiple comparisons test, as well as regression analysis (GraphPad Prism 3.0; $p < 0.05$).

Results

Adult Human White Matter Progenitor Cells

Expressed Oligodendrocyte Progenitor Marker Genes

Adult human subcortical WMPCs were enriched by MACS using the A2B5 marker as described previously.^{1,2} Of the 18 patient samples used in this study, 4 were used for genomic analysis, and 14 for in vitro analysis. From each sample, we obtained between 3×10^5 and 1×10^6 A2B5⁺ cells that comprised roughly 3% of all viably dissociated white matter cells. To identify those genes whose expression distinguished the A2B5⁺ WMPC population from other cell types present in normal adult white matter, we performed microarray analysis on both RNA extracted from WMPCs immediately after sorting, and RNA extracted from the original dissociates from which the sorts were derived. Beginning with at least 100ng of total RNA per isolate, we performed two rounds of RNA ampli-

Table 1. Marker Gene Expression Profile of A2B5⁺ White Matter Progenitor Cells

Cell Type	Symbol (Name)	Array Ratio	qPCR Ratio
Oligodendrocyte progenitor	CSPG4 (NG2)	19.41 ± 2.62 ($p = 3 \times 10^{-5}$)	15.05 (13.66–16.57; $p < 0.001$) ^a
	PDGFRA	11.18 ± 0.89 ($p = 7 \times 10^{-6}$)	22.67 (19.30–26.61; $p < 0.001$)
Oligodendrocytic	ST8SIA1 (GD3 synthase)	5.25 ± 0.89 ($p = 6 \times 10^{-4}$)	9.39 (8.62–10.23; $p < 0.01$)
	CNP (CNPase)	1.64 ± 0.21	
	NKX2-2	1.53 ± 0.42	
	OLIG2	1.71 ± 0.39	
	PLP1 (PLP/DM20)	1.21 ± 0.19	
	QKI	1.06 ± 0.29	
	SOX10	1.19 ± 0.26	
Myelinating oligodendrocytic	GALC	1.07 ± 0.20	
	MAG	1.22 ± 0.24	
	MAL	0.81 ± 0.14	
	MBP	1.32 ± 0.23	
	MOBP	0.28 ± 0.15	
	MOG	0.52 ± 0.25	
Astrocyte	AQP4	1.37 ± 0.98	
	AQP9	0.29 ± 0.19	
	GFAP	1.70 ± 0.33	
	GLUL (glutamine synthase)	0.86 ± 0.15	
	S100B	1.00 ± 0.14	
	TNC (Tenascin C)	1.40 ± 1.14	
	ASCL1 (MASH1)	12.32 ± 1.72 ($p = 6 \times 10^{-5}$)	18.67 (15.97–21.82; $p < 0.05$)
Neural progenitor/stem cell ^a	DCX (doublecortin)	7.56 ± 2.91	
	HES1	5.13 ± 1.27 ($p = 0.0027$)	12.52 (11.86–13.21; $p < 0.001$)
Neuron ^a	ELAVL3 (HuC)	1.13 ± 0.19	
	ELAVL4 (HuD)	2.50 ± 0.54	
	MAP2	0.92 ± 0.49	
	MAP2 (alternate probe)^a	4.17 ± 0.56 ($p = 0.0005$)	
	NEF3 (neurofilament med)	1.33 ± 0.13	
	TUBA3 (T α 1 tubulin)	0.84 ± 0.16	
Endothelial ^a	CDH5 (VE-Cadherin)	0.58 ± 0.20	
	TEK (TIE2)	0.82 ± 0.56	
	CD68	0.49 ± 0.12	
Microglial	CD86	0.27 ± 0.40	
	HLA-DRA	0.22 ± 0.14	
	HLA-DRB1	0.22 ± 0.12	

Expression of cell-type marker genes in the white matter progenitor cells (WMPCs) was calculated by normalization of each sorted profile against the matched unsorted dissociate. We examined a set of more than 50 genes whose expression can be used to discriminate neural cell populations in the adult brain. Only genes with reliably detected expression, that is, probe sets with at least one present call, are shown. For genes with multiple probe sets we have shown the probe set with the most significant ratio of expression. Only those genes expressed by oligodendrocyte and less restricted neural progenitors were significantly expressed in WMPCs, compared with their environment (in bold). These data were confirmed by quantitative polymerase chain reaction (qPCR) analysis. The C_t values of sorted WMPCs and the unsorted dissociate was compared following normalization to 18S ribosomal RNA, and significance was assessed by paired t test statistics. Mean ratio of expression and standard error were calculated using the C_t differences, and the anti-log values are shown for comparison with probe set data.

Other markers considered, SOX1, DLX2/5, NEFL (neurofilament light), and vWF (von Willebrand factor), were not detected in either A2B5⁺ WMPCs or unsorted white matter cells, but were found in human fetal VZ tissue (data not shown).

Details of primers/probes used for real-time PCR analysis are available in the supplementary information (see Supplementary Table 3).

^aAn alternatively sliced version of MAP2 has been shown to be expressed by oligodendrocyte progenitors and then downregulated during differentiation.⁵⁸

fication prior to hybridization to Affymetrix HG-U95Av2 GeneChips, using Affymetrix's small sample protocol. Following microarray-wide normalization, the expression of individual genes in each WMPC isolate was normalized against that of the unsorted white matter dissociate from which it was derived, and the mean expression ratio was calculated from the individual samples.

To analyze the microarray data, we first examined the expression of several marker genes expressed by glial progenitor cells in lower species (Table 1). The antibody we used to isolate adult WMPCs, monoclonal A2B5,^{1,9,10} recognizes the G_Q and G_{T3} gangliosides and their O-acetylated derivatives.¹¹ We found that the expression of GD3 synthase (ST8SIA1), the enzyme that catalyzes the transfer of sialic acid from CMP-

sialic acid to GM3, and by which GD3 and GT3 are generated, was significantly enriched in the WMPC pool. This observation was confirmed with real-time reverse transcriptase PCR analysis (qPCR) of GD3 synthase mRNA levels, following normalization to 18S ribosomal RNA and the unsorted controls ($\Delta\Delta C_t$ analysis, paired t test, $p < 0.01$; see Table 1). Furthermore, microarray analysis showed strong expression of PDGFRA and NG2 (chondroitin sulfate proteoglycan 4 [CSPG4]), two prototypic markers of oligodendrocyte progenitors *in vivo*, which we confirmed by qPCR (see Table 1). Two oligodendrocyte lineage basic helix-loop-helix transcription factors, Olig2 and Nkx2.2,¹² were also detected in the WMPC profile. However, neither gene was significantly enriched compared with unsorted white matter, presumably because mature oligodendrocytes also express Olig2 and Nkx2.2.^{13,14} Similarly, more mature oligodendrocytic transcripts, including CNP and the myelin genes myelin basic protein (MBP) and proteolipid protein (PLP1), were underexpressed by WMPCs relative to their parental white matter. Markers of other white matter phenotypes, namely, astrocytes, microglia, and endothelial cells, were either unenriched or relatively depleted in WMPCs (see Table 1). Thus, the transcriptional profile of A2B5-sorted WMPCs exhibited the differential expression of a number of genes previously associated with oligodendrocyte progenitor cells.

Interestingly, several markers of early neural cell growth and migration were noted to be differentially expressed by WMPCs. Doublecortin (DCX), which is expressed by migrating immature cells during development, was more than eightfold enriched in WMPCs. GAP43, a growth and regeneration-associated marker of process extension, was enriched more than fourfold in WMPCs, confirming earlier reports of the expression of GAP43 by rodent oligodendrocyte progenitors.¹⁵ GAD67 mRNA, which encodes glutamate decarboxylase and as such serves as a marker of γ -aminobutyric acid (GABA) production, was enriched more than eightfold in A2B5-sorted WMPCs. Although GABA expression has previously not been described in oligodendrocyte lineage cells, glutamate decarboxylase expression by these progenitor cells might have reflected their potential to generate GABAergic neurons when cultured in low density.²

Adult White Matter Progenitor Cells Are Transcriptionally Distinct from the Local White Matter Environment

The Affymetrix U95Av2 GeneChip analyzes the expression of approximately 8,500 genes. Fifty-three percent and 56% of these genes were respectively detected in RNA extracted from the A2B5-sorted WMPCs and the unsorted dissociates from which they derived. The degree of overlap was large; 92% of those genes ex-

pressed in the A2B5-sorted pool were also detected in the unsorted dissociate. We then identified a set of genes whose expression was significantly enriched in the A2B5-sorted WMPC-enriched population, compared with the unsorted white matter dissociate. Using GeneSpring (Silicon Genetics) to analyze the array database, we first removed those Affymetrix probe sets that were deemed “absent” in all three A2B5-sorted profiles. The remainder, comprising reproducibly hybridized oligonucleotides, were then used to generate a list of probe sets the expression of which was significantly higher in sorted cells than in the unsorted dissociate, as assessed by paired t tests (see Materials and Methods). The resulting list of 159 probe sets (<5% of total) was then pruned by removing those that were either ambiguously annotated as mapping to multiple genes, or that were novel, by virtue of not yet having been annotated to the National Center for Biotechnology Information with Entrez GeneID identifiers. The remaining probe sets were annotated to 132 distinct genes (Table 2; see also the complete list that is available via the Internet at: www.urmc.rochester.edu/goldmanlab/sim2005.htm). For each identified gene, additional probe sets were then identified. Transcripts depleted from the A2B5-sorted WMPC-enriched population were determined by the same analysis procedure, by inverting the expression ratios of the A2B5-sorted pool. The number of depleted transcripts was larger than the number selectively enriched, with 507 probe sets identified that mapped to 471 distinct genes (the complete list is available at: www.urmc.rochester.edu/goldmanlab/sim2005.htm).

We next examined the frequency of functionally related transcripts to determine relevant functional categories of genes. Overrepresented functional categories in the A2B5-sorted WMPC cell profile were determined by comparison with the entire population of genes on the HG-U95Av2 microarray. Using the EASE software tool¹⁶ to examine the Gene Ontology (GO) biological process annotation (www.geneontology.org) of WMPC-enriched genes, we found that genes belonging to the neurogenesis, cell adhesion, and cell communication categories were overrepresented ($p < 0.05$, EASE score/adjusted Fisher’s exact test with post hoc comparisons; see Supplementary Table 1). In contrast, when we performed the same analysis on genes *depleted* from the WMPC pool, we found that genes involved in immune and inflammatory responsiveness were selectively depleted from sorted WMPCs (see Supplementary Table 2).

White Matter Progenitor Cells Expressed a Cohort of Receptors Suggesting Active Environmental Interrogation

Belying their apparent relative quiescence, adult WMPCs were found to differentially express a set of

Table 2. Functionally Relevant Genes Are Highly Expressed by White Matter Progenitor Cells

HUGO Symbol	Common Name/Description	NCBI GeneID	Expression Ratios	<i>p</i>
Ligands, antagonists, and secreted proteins				
CHRDL1	Neuralin 1; Ventroptin	91851	14.46 ± 5.63	2.4 × 10 ⁻³
SCG2	Secretogranin II (chromogranin C)	7857	11.02 ± 3.63	1.9 × 10 ⁻³
CHGB	Chromogranin B (secretogranin 1)	1114	7.55 ± 1.16	2.0 × 10 ⁻⁴
SERPINE2	Glia-derived nexin	5270	5.81 ± 1.52	2.5 × 10 ⁻³
BMP7	OP-1	655	4.93 ± 1.18	2.6 × 10 ⁻³
NELL2	NEL-like 2 (chicken), NRP2	4753	4.48 ± 0.78	9.9 × 10 ⁻⁴
PTN	Pleiotrophin; HB-GAM	5764	4.18 ± 0.37	8.2 × 10 ⁻⁵
TIMP4	Tissue inhibitor of metalloproteinase 4	7079	3.92 ± 0.72	1.8 × 10 ⁻³
BMP2	Dpp homologue	650	2.95 ± 0.25	2.2 × 10 ⁻⁴
SLIT1	Slit homolog 1 (Drosophila)	6585	2.76 ± 0.20	1.4 × 10 ⁻⁴
HTRA1	Protease, serine, 11 (insulin-like growth factor [IGF] binding)	5654	2.06 ± 0.15	5.6 × 10 ⁻⁴
Receptors and downstream components				
GRIK2	Glutamate receptor, ionotropic, kainate 2	2898	30.54 ± 8.53	2.6 × 10 ⁻⁴
SLC1A2	Glial high-affinity glutamate transporter	6506	22.66 ± 5.95	2.9 × 10 ⁻⁴
SH2D1A	SH2 domain protein 1A, Duncan's disease	4068	21.51 ± 7.20	7.9 × 10 ⁻⁴
GRIK1	Glutamate receptor, ionotropic, kainate 1	2897	17.76 ± 4.88	4.7 × 10 ⁻⁴
ADCY8	Adenylate cyclase 8 (brain), ADCY3, HBAC1	114	17.29 ± 7.10	2.3 × 10 ⁻³
CAP2	Adenylyl cyclase-associated protein 2	10486	16.75 ± 5.60	1.1 × 10 ⁻³
TSPAN7	Transmembrane 4 superfamily member 2	7102	11.45 ± 2.31	2.7 × 10 ⁻⁴
PDGFRA	Platelet-derived growth factor receptor-α	5156	11.18 ± 0.89	6.9 × 10 ⁻⁶
KCNB1	Potassium voltage-gated channel, Shab-like	3745	9.11 ± 2.19	7.8 × 10 ⁻⁴
GABRB1	γ-Aminobutyric acid (GABA) A receptor	2560	8.69 ± 2.09	8.5 × 10 ⁻⁴
GLRB	Glycine receptor-β	2743	7.82 ± 2.17	1.8 × 10 ⁻³
ATP1A2	ATPase, Na ⁺ /K ⁺ transporting, α2	477	5.71 ± 0.56	5.9 × 10 ⁻⁵
CNR1	Cannabinoid receptor 1 (brain)	1268	5.31 ± 0.75	2.9 × 10 ⁻⁴
APOD	Apolipoprotein D	347	5.26 ± 0.85	5.2 × 10 ⁻⁴
PDGFRA _{variant}	1.5kb alternate PDGFRA truncated transcript	5156	5.16 ± 0.98	9.8 × 10 ⁻⁴
DOK5	Docking protein 5	55816	4.36 ± 0.70	7.7 × 10 ⁻⁴
GRIA2	Glutamate receptor, ionotropic, AMPA 2	2891	4.03 ± 0.28	3.5 × 10 ⁻⁵
ERBB4	v-erb-a erythroblastic leukemia viral 4	2066	3.72 ± 0.54	8.1 × 10 ⁻⁴
KCND3	Potassium voltage-gated channel, Shal-like	3752	3.67 ± 0.33	1.4 × 10 ⁻⁴
ACCN2	Neuronal amiloride-sensitive cation channel 2	41	3.30 ± 0.52	1.6 × 10 ⁻³
LDLR	Low-density lipoprotein receptor	3949	3.21 ± 0.33	3.5 × 10 ⁻⁴
TNK2	Activated p21cdc42Hs kinase	10188	3.13 ± 0.19	4.6 × 10 ⁻⁵
GPR19	G-protein-coupled receptor 19	2842	2.82 ± 0.23	2.3 × 10 ⁻⁴
MAGED1	NRAGE, DLXIN1	9500	2.29 ± 0.17	3.3 × 10 ⁻⁴
CASK	Calcium/calmodulin-dependent serine kinase	8573	2.20 ± 0.23	1.5 × 10 ⁻³
RAB31	RAB31, member RAS oncogene family	11031	2.05 ± 0.21	2.3 × 10 ⁻³
Cell adhesion and extracellular matrix molecules				
CSPG4	NG2	1464	19.41 ± 2.62	2.5 × 10 ⁻⁵
TNR	Tenascin R (restrictin, janusin)	7143	14.66 ± 0.75	7.8 × 10 ⁻⁷
OPCML	Opioid binding protein/cell adhesion molecule-like	4978	13.87 ± 3.28	3.7 × 10 ⁻⁴
CLDN10	Claudin 10	9071	13.63 ± 5.00	2.1 × 10 ⁻³
NRCAM	Neuronal cell adhesion molecule	4897	13.62 ± 2.77	2.1 × 10 ⁻⁴
CHL1	Close homolog of L1CAM	10752	11.80 ± 3.96	1.8 × 10 ⁻³
GPM6A	Glycoprotein M6A	2823	9.21 ± 1.22	7.3 × 10 ⁻⁵
COL11A1	Collagen, type XI, alpha 1	1301	9.14 ± 2.80	1.9 × 10 ⁻³
PTPRZ1	RPTPζ/phosphocan	5803	8.74 ± 0.30	3.5 × 10 ⁻⁷
CSPG2	Versican	1462	8.36 ± 0.69	1.4 × 10 ⁻⁵
DSCAM	Down's syndrome cell adhesion molecule	1826	6.94 ± 0.71	4.7 × 10 ⁻⁵
CSPG5	Neuroglycan C/NGC	10675	6.88 ± 1.18	3.6 × 10 ⁻⁴
THBS4	Thrombospondin 4	7060	6.15 ± 0.66	7.1 × 10 ⁻⁵
CSPG3	Neurocan	1463	5.66 ± 0.43	2.2 × 10 ⁻⁵
FLRT2	Fibronectin leucine rich transmembrane protein 2	23768	5.11 ± 0.66	2.3 × 10 ⁻⁴
PCDH8	Protocadherin 8, PAPC, Arcadlin	5100	4.79 ± 1.10	2.4 × 10 ⁻³
ASTN	Astrotactin	460	4.40 ± 0.57	3.3 × 10 ⁻⁴
BGN	Biglycan	633	3.12 ± 0.32	3.8 × 10 ⁻⁴
SDC3	Syndecan 3 (N-syndecan)	9672	2.69 ± 0.34	1.4 × 10 ⁻³

Table 2. Continued

HUGO Symbol	Common Name/Description	NCBI GeneID	Expression Ratios	<i>p</i>
NLGN1	Neuroigin 1	22871	2.64 ± 0.29	9.2 × 10 ⁻⁴
NCAM1	NCAM	4684	2.51 ± 0.16	1.5 × 10 ⁻⁴
PCDH21	MT-protocadherin	92211	1.96 ± 0.17	1.3 × 10 ⁻³
THBS2	Thrombospondin 2	7058	1.89 ± 0.17	2.3 × 10 ⁻³
Transcription factors and Regulators				
SOX5	SRY (sex determining region Y)-box 5	6660	15.69 ± 3.75	3.2 × 10 ⁻⁴
ASCL1	MASH1	429	12.32 ± 1.72	5.6 × 10 ⁻⁵
FOXP1B	BF1	2290	10.29 ± 3.49	2.3 × 10 ⁻³
LHX2	LIM homeobox protein 2, LH - 2	9355	9.50 ± 2.81	1.6 × 10 ⁻³
ETV1	Ets variant gene 1/ER81	2115	8.51 ± 2.34	1.5 × 10 ⁻³
HES1	Hairy and enhancer of split 1	3280	5.13 ± 1.27	2.7 × 10 ⁻³
FHL1	SLIM1	2273	4.50 ± 0.65	4.9 × 10 ⁻⁴
MYC	v-myc/c-myc	4609	3.81 ± 0.36	1.5 × 10 ⁻⁴
HLF	Hepatic leukemia factor	3131	3.55 ± 0.35	2.0 × 10 ⁻⁴
JUN	c-JUN	3725	2.89 ± 0.16	3.9 × 10 ⁻⁵
SATB1	Special AT-rich sequence binding protein 1	6304	2.86 ± 0.35	9.7 × 10 ⁻⁴
C1orf61	Transcriptional activator of the c-fos promoter	10485	2.77 ± 0.32	9.3 × 10 ⁻⁴
SOX4	SRY (sex determining region Y)-box 4	6659	2.72 ± 0.37	1.8 × 10 ⁻³
NR2F1	COUP-TFI	7025	2.72 ± 0.26	5.1 × 10 ⁻⁴
NFIB	Nuclear factor I/B	4781	2.35 ± 0.22	7.8 × 10 ⁻⁴
SMARCD3	SWI/SNF related, matrix associated	6604	2.18 ± 0.26	2.8 × 10 ⁻³
FOS	v-fos FBJ murine osteosarcoma oncogene	2353	2.04 ± 0.19	1.5 × 10 ⁻³
SOX18	SRY (sex determining region Y)-box 18	54345	1.77 ± 0.14	2.2 × 10 ⁻³

Gene expression profiles of A2B5⁺ sorted white matter progenitor cells (WMPCs) were normalized to the unsorted dissociate from which each was derived. A paired *t* test was performed on reliably detected genes using a false discovery rate of 10% to mitigate for multiple testing. The list of 132 significantly enriched genes was then grouped according to gene ontology. Genes not falling into ligand, receptor, cell adhesion, and transcription factors categories were omitted from this table (the complete list is available via the Internet at: www.urmc.rochester.edu/goldmanlab/sim2005.htm). For genes with multiple Affymetrix probe sets (Affymetrix, Santa Clara, CA), we used the probe set with the most significant ratio of expression. The level of expression compared with unsorted dissociate is shown with standard errors.

NCBI = National Center for Biotechnology Information.

receptors that would permit their responsiveness to a wide variety of growth factors and neurotransmitters (see Table 2). Among receptor tyrosine kinases, PDGFRA was one of the most significantly enriched annotated genes - by 11.2-fold - found in WMPCs (see Table 1). In addition to full length PDGF α R, a truncated PDGFRA splice variant missing the extracellular ligand-binding domain¹⁷ was also enriched in WMPCs (see Table 2). Another receptor class previously implicated in oligodendrocyte progenitor ontology,^{18,19} the erbB receptors of the neuregulins, were represented by erbB3 and erbB4, both of which were expressed by adult WMPCs, erbB4 differentially so (see Table 2). A number of other tyrosine kinases, including type 1 fibroblast growth factor receptor (FGFR1), insulin receptor (INSR), insulin-like growth factor-1 receptor, and TrkB (NTRK2), were expressed by WMPCs, although no more so than by their surrounding white matter. Similarly, FGFR3, the high-affinity receptor for FGF1, FGF4, and FGF9, was also highly expressed by sorted WMPCs (10.21 ± 4.54, relative to unsorted dissociate), in accord with prior descriptions of its role in oligodendrocytic maturation.²⁰ However, the expression of FGFR3 in the white matter surround was also

high, likely on account of oligodendrocytic expression, so that it did not achieve significance as differentially expressed by WMPCs.

Besides these receptor tyrosine kinases, several G-protein-coupled receptors were differentially expressed by adult human WMPCs. These included the relatively uncharacterized GPR19 and the cannabinoid receptor 1 (CNR1),²¹ confirmed by qPCR (Table 3). In addition, we identified a single relatively uncharacterized adenylyl cyclase, ADCY8, as highly differentially expressed, by more than 17-fold relative to unsorted white matter (see Table 2). Sorted WMPCs also selectively expressed high levels of surface receptors for several neurotransmitters, including ionotropic as well as metabotropic receptors for GABA, glutamate, and glycine (see Table 2). This suggests a high degree of responsiveness to the local transmitter environment and, in particular, a greater activity-dependent responsiveness than might have been expected from a nominally quiescent phenotype. Although the normal role of these receptors in the maintenance of adult WMPCs is unclear, their differential expression provides us a set of potential drug targets, the modulation of which may

Table 3. Quantitative Polymerase Chain Reaction Validation of Functionally Relevant Genes Expressed by White Matter Progenitor Cells

Ontology	HUGO Symbol (Name)	qPCR Expression Ratio	Standard Error Range	p (<i>t</i> test)
Notch pathway	MASH1	18.67	15.97–21.82	$p < 0.05$
	HES1	12.52	11.86–13.21	$p < 0.001$
	FHL1	10.81	6.62–17.64	$p < 0.05$
	FHL1B (RBP-J binding)	9.19	6.51–12.99	$p < 0.01$
	JAG1 (jagged 1)	2.76	2.53–3.02	$p < 0.01$
	NOTCH1	1.59	1.50–1.70	$p < 0.05$
	MSI1 (musashi 1)	10.09	7.31–13.93	n = 2, NS ^a
	RBPSUH (RBP-J)	1.00	0.78–1.29	n = 3, NS
RTPZ and syndecan pathways	PTPRZ1 (RTPZ)			
	Both R isoforms	15.62	10.43–23.38	$p < 0.01$
	Short R isoform	9.38	6.80–12.94	n = 2, NS ^a
	Long R isoform	27.94	22.52–34.66	$p < 0.001$
	PTN (pleiotrophin)	4.42	3.72–5.25	$p < 0.01$
	SDC3 (syndecan-3)	7.22	5.92–8.81	$p < 0.01$
	CASK	4.66	4.15–5.22	$p < 0.001$
Other signal pathways	PDGFRA	22.67	19.30–26.61	$p < 0.001$
	CHRD1	20.55	17.06–24.76	$p < 0.05$
	CNR1	10.92	7.76–15.38	$p < 0.01$

Expression of selected enriched genes was validated by real-time reverse transcriptase polymerase chain reaction analysis, shown above grouped according to signal pathway; significantly enriched genes are in bold. Following normalization to 18S ribosomal RNA, the ΔC_t values of sorted white matter progenitor cells (WMPCs) and the unsorted dissociate were compared and significance assessed by paired *t* test statistics. Following anti- \log_2 transformation, mean ratios of expression and ± 1 standard error ranges were calculated from $\Delta\Delta C_t$ values.

^aMSI1 and PTPRZ1 short R-isoform primers did not amplify in two of the unsorted samples by qPCR, preventing calculation of an appropriate ratio in these samples and therefore reducing the sample number. RTPZ = receptor tyrosine phosphatase- β/ζ ; NS = not significant.

permit us to selectively influence the turnover and fate of these cells.

White Matter Progenitor Cells Expressed Both Receptor Tyrosine Phosphatase β/ζ and Its Ligand, Pleiotrophin

Among receptor tyrosine phosphatases, RTPZ was highly expressed and differentially so, as were most of its known ligands (see below). In fact, RTPZ was the single-most significantly enriched receptor-encoding gene in our analysis, and it was more than 15-fold enriched in WMPCs relative to unsorted cells by qPCR (see Table 2; $p < 0.01$). The Affymetrix probe set and qPCR primers were specific for the intracellular phosphatase domain of RTPZ, as opposed to its secreted ectodomain, phosphacan. To distinguish between the short and long receptor isoforms of RTPZ, we designed specific qPCR primers for each. Although both receptor isoforms were significantly more expressed in the WMPCs, the longer isoform containing the glycosaminoglycan side chains was more than 25-fold enriched in WMPCs ($p < 0.001$; see Table 3).

Importantly, the only known soluble ligand of RTPZ, pleiotrophin (PTN),⁸ was also found to be expressed significantly higher in the WMPC-enriched profile by both microarray and qPCR analysis (see Tables 2 and 3). Besides binding RTPZ, PTN has also

been shown to bind the syndecan family of transmembrane heparin-sulphate proteoglycans. Interestingly then, syndecan-3 (SDC3) mRNA was also differentially expressed by sorted adult human WMPCs, as has been reported in rat oligodendrocyte progenitors²² (see Tables 2 and 3).

Inhibition of Tyrosine Phosphatase Activity Induces Oligodendrocyte Differentiation in White Matter Progenitor Cells

Because of the high expression of the tyrosine phosphatase receptor RTPZ in WMPCs, we asked whether receptor tyrosine phosphatase inhibition might influence the differentiation of WMPCs. bpV(phen), a known potent inhibitor of tyrosine phosphatase activity,²³ was used to induce inhibition. Cultures exposed for 7 days to 25ng/ml bpV(phen) exhibited significantly less maintenance of A2B5⁺ cells compared with untreated control cultures ($4 \pm 0.5\%$ vs $15 \pm 2.2\%$; n = 4 patients; Fig 1A). In contrast, both the incidence and net proportion of O4⁺ cells increased dramatically in these bpV(phen)-treated cultures ($54 \pm 17.6\%$ vs $20 \pm 8.4\%$; see Figs 1A, C, D). As a result, the O4/A2B5 ratio in these cultures increased in response to bpV(phen) in a dose-dependent fashion, from less than 10% to more than 70%. When the respective proportions of A2B5⁺ and O4⁺ cells were plotted as a

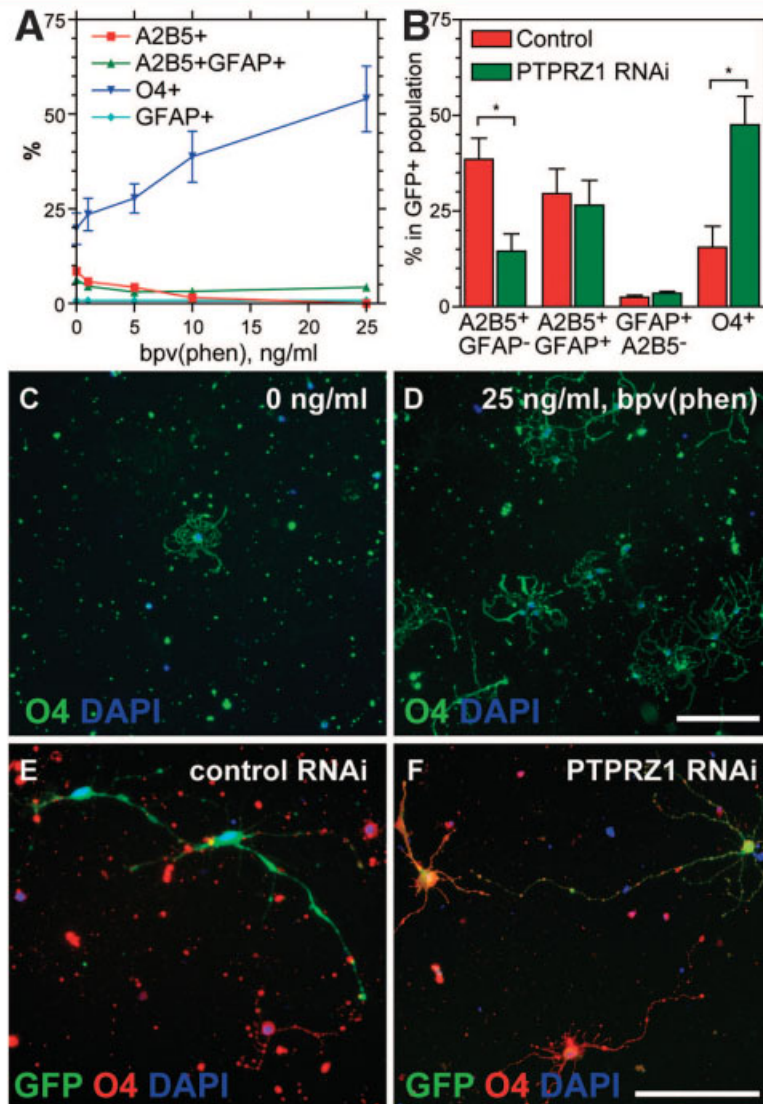


Fig 1. Receptor tyrosine phosphatase- β/ζ (RTPZ) inhibition induces oligodendrocyte differentiation by adult white matter progenitor cells (WMPCs). (A) Dose–response curves and linear regressions thereof of the proportion of A2B5-defined progenitors versus O4-defined oligodendrocytes as a function of Potassium bisperoxo(1,10-phenanthroline)oxovanadate (V) (bpV(phen)) dose. (B) Plots of the respective incidences of A2B5⁺ progenitors and O4⁺ oligodendrocytes as a function of lentiviral RTPZ RNAi treatment (\pm standard error of the mean; $n = 4$). (C, D) WMPCs were treated with 0 or 25ng/ml bpV(phen) for 7 days in vitro; matched wells were then stained for either A2B5 (C) or O4 (D). (E, F) WMPCs were treated with lentiviral RTPZ RNAi; a week later, matched wells were then stained for A2B5 (E) or O4 (F). Asterisk indicates significant difference, $p < 0.01$. Scale bar = 10 μ m. GFAP = glial fibrillary acidic protein; GFP = green fluorescent protein; DAPI = 4'6-diamidino-2-phenylindole.

function of dose, regression lines were generated, the slopes of which differed significantly ($p = 0.008$, two-tailed t test on four paired samples). Similarly, two-way ANOVA of the incidence of A2B5⁺ and O4⁺ cells as function of bpV(phen) dose showed a significant dose-dependent suppression of the A2B5 phenotype and expansion of O4⁺ cells ($p < 0.0001$; $F = 74.4$ [1, 4 degrees of freedom (df)]). Post hoc analysis showed that the pbV(phen) dose-dependent change in the relative proportions of A2B5⁺ and O4⁺ cells achieved statistical significance at 5ng/ml ($p < 0.05$). Moreover,

the total cell number was unaffected by dosage levels over the range of 1 to 25ng bpV(phen), as was the proportion of BrdU⁺ A2B5⁺ cells (data not shown), suggesting that the effect of bpV(phen) treatment was due to induction of oligodendrocyte differentiation.

Lentiviral Receptor Tyrosine Phosphatase- β/ζ shRNAi Induces Oligodendrocytic Differentiation of White Matter Progenitor Cells

To further establish the specificity of RTPZ in tyrosine phosphatase inhibition-induced differentiation, we de-

veloped an RNAi knock-down vector specific for the long receptor isoform of RTPZ (see Materials and Methods section earlier in article; see also the Supplementary Fig). Following lentiviral shRNAi infection of WMPCs, the GFP⁺ transductants significantly differentiated as O4⁺ oligodendrocytes at 14 days in vitro ($15 \pm 4\%$ vs $48 \pm 5.1\%$; $p = 0.0017$ [2 df], paired t test) and exhibited a marked reduction in A2B5⁺GFAP⁻ progenitor production and expansion ($38 \pm 4.2\%$ vs $15 \pm 3.6\%$; $p = 0.0062$ [2 df], paired t test; see Fig 1B). The proportion of O4⁺ oligodendrocytes or A2B5⁺ GFAP⁻ progenitors in the GFP-negative (untransduced) pool did not differ between control and lentiviral RTPZ RNAi-infected populations, suggesting that the effect of RTPZ knock-down was cell autonomous. Furthermore, the total cell number remained constant between control and RTPZ RNAi-infected populations (data not shown). Thus, the suppression of RTPZ promotes the direct oligodendrocytic differentiation of adult human WMPCs.

White Matter Progenitor Cells Express Surface Adhesion Molecules That May Interact with Receptor Tyrosine Phosphatase- β/ζ

The differential expression by WMPCs of both PTN and its two known receptors, RTPZ and syndecan, suggested the wisdom of further investigating both RTPZ and syndecan binding partners in these cells. Previous studies have shown that syndecan is subject to regulated intramembrane proteolysis that leads to the release of the transcriptional regulator calmodulin-activated serine kinase (CASK) from the cytoplasmic domain of syndecan.²⁴ Once released by syndecan, CASK translocates to the nucleus, where it can activate the T-box family transcription factor TBR1, inducing transcription of T-box target genes.²⁵ We found that CASK was indeed significantly enriched in WMPCs in both our microarray and qPCR analyses (see Tables 2 and 3), suggesting the competence of this regulatory pathway in adult WMPCs.

We next asked whether WMPCs were enriched in RTPZ's binding partners. Although PTN is the only known soluble ligand for RTPZ, among other RTPZ binding partners, the extracellular matrix glycoprotein tenascin-R (TNR)²⁶ and CAM family members NrCAM²⁷ and NCAM1²⁸ were also differentially expressed by isolated WMPCs (see Table 2). Indeed, virtually every described heterophilic ligand of RTPZ was represented, highlighting the likely importance of *cis* regulation of RTPZ and RTPZ-dependent signaling to the maintenance of WMPCs. Because RTPZ is able to mediate the dephosphorylation of β -catenin, and thereby permits catenin's nuclear translocation and catenin-dependent transcriptional activation,⁸ it is likely that RTPZ's binding partners may act to modu-

late the basal phosphorylation state of β -catenin in these cells.

Cell-Cell Adhesion and Extracellular Matrix Molecules of Adult Human White Matter Progenitor Cells

A cohort of 23 transcripts encoding known and putative cell adhesion molecules were enriched in WMPCs (Gene Ontology accession, GO:0007155). These included members of the cadherin, CAM, CSPG, and tenascin gene families (see Table 2). Of specific interest, the L1-family member CHL1 was strongly overexpressed by WMPCs. CHL1 has been shown to be expressed by rat oligodendrocyte progenitors in vitro,²⁹ and previous studies have highlighted the role of L1-dependent calcium signaling in modulating the migration and survival of early neural progenitor cells.^{30,31} Yet the related CAM family molecule NrCAM may be of even greater interest here, because it has been shown to act as a heterophilic ligand for the RTPZ ectodomain.²⁷

Importantly, the matrix molecule TNR was the second most significantly enriched gene in the A2B5-sorted WMPC pool (see Table 2). TNR has been shown to be expressed by rodent A2B5⁺ oligodendrocyte progenitors in vitro and may regulate their lineage progression.³² Like NrCAM, TNR also binds to the RTPZ ectodomain,²⁶ and it is necessary for the normal distribution of RTPZ in white matter.³³

Besides the well-characterized RTPZ binding molecules, four CSPGs were differentially expressed by human WMPCs. These included versican (CSPG2), neurocan (CSPG3), NG2 (CSPG4), and neuroglycan C (CSPG5); each was enriched by 5- to 20-fold in A2B5-sorted WMPCs (see Table 2). In addition to NG2, rodent oligodendrocyte progenitors had previously been shown to express versican³⁴ and neurocan.³⁵ Yet neuroglycan C, a member of the aggrecan family localized to the brain, had not previously been reported to be expressed by oligodendrocyte progenitors. Remarkably then, essentially all known brain CSPGs were differentially expressed by adult WMPCs, at many-fold higher levels than the white matter from which they derived.

White Matter Progenitor Cells Differentially Expressed Notch-Regulated Transcripts

Besides genes characteristic of oligodendrocyte progenitors, a number of transcripts associated with less committed and early neural phenotypes were also differentially expressed by adult human WMPCs. In particular, two transcription factors typical of neural progenitors and stem cells, respectively, MASH1 (ASCL1) and HES1, were highly enriched by these cells (see Table 1). MASH1 expression was 12-fold greater by microarray, and more than 18-fold by qPCR, in A2B5⁺ cells relative to the unsorted white matter from which they

were extracted (see Table 3). HES1 was 5-fold higher by microarray, and more than 12-fold higher by qPCR. Importantly, both MASH1 and HES1 are downstream components of the notch signaling pathway, which has already been noted to regulate oligodendrocyte progenitor differentiation in the rat optic nerve.³⁶ Accordingly, a number of other notch-signaling components were expressed in WMPCs. Because the Affymetrix U95Av2 chip does not contain probe sets to NOTCH1, we determined whether WMPCs expressed notch receptor by qPCR. NOTCH1 expression was 60% higher in WMPCs than the unsorted white matter dissociate ($p < 0.05$; see Table 3). NOTCH2/3 were not detected in either the WMPCs or the unsorted dissociate; NOTCH4, although present, was not enriched in the WMPCs. Although notch ligands are poorly represented on the microarray, jagged1 (JAG1) was detected in both WMPCs and the unsorted dissociate (see Table 3). Surprisingly, qPCR analysis showed that WMPCs express significantly more JAG1 than their surrounding white matter environment ($p < 0.01$), suggesting the capacity for lateral inhibition of differentiation among contiguous WMPCs.

Notch signaling typically activates transcription through CBF/RBP-J, which in turn upregulates HES1 expression. In this regard, we noted that four and a half LIM domains (FHL1), a novel RBP-J binding protein,³⁷ was also significantly enriched in sorted WMPCs. We found significant expression of FHL1 by microarray, and qPCR demonstrated that the FHL1B RBP-J binding splice variant was enriched more than 10-fold ($p < 0.05$; see Table 3). We similarly noted high and differentially expressed levels of the mRNA encoding musashi1, an RNA-binding protein that binds the 3' untranslated region of numb mRNA; musashi mediates the down-regulation of numb protein, thereby relieving numb-mediated inhibition of notch.³⁸ In WMPCs, although we found only low levels of NUMB mRNA, the level of musashi1 mRNA was much greater in the sorted WMPCs than in unsorted white matter cells (see Table 3). This was consistent with the tonic activation of notch signaling in adult human WMPCs, just as in neural stem cells and glial progenitors in early development.^{36,39}

Components of the Bone Morphogenetic Protein Signaling Pathway Were Expressed by White Matter Progenitor Cells

Apart from notch signaling, we also found evidence for activation and antagonism of the BMP signaling pathway in WMPCs. Both BMP2 and BMP7 were significantly enriched in WMPCs by three-fold and five-fold, respectively (see Table 2). Yet along with overexpression of these BMP ligands, neuralin/ventropin (CHRDL1), a selective antagonist of BMP4,⁴⁰

was also noted to be highly expressed. We confirmed this observation by qPCR, by which CHRDL1 was more than 20-fold higher in WMPCs ($p < 0.05$). In addition, we found high expression of BAMBI (BMP and activin membrane-bound inhibitor), a membrane-tethered negative regulator of BMP signaling.⁴¹ (BAMBI's differential expression was high but variable, and thus did not achieve significance at a 10% false discovery rate, although it did at more liberal acceptance levels.) These data may suggest an autocrine support of WMPC maintenance by BMP2- and BMP7-dependent pathways, with a concurrent inhibition of alternative BMPs by neuralin and BAMBI.

Bone Morphogenetic Protein 4 Selectively Induces Astrocytic Differentiation in White Matter Progenitor Cells

To test the specific importance to cell fate determination of BMP4 signaling, and hence of its tonic inhibition by BAMBI and neuralin, we challenged WMPCs with exogenous BMP4, as well as with the two BMP ligands that WMPCs were noted to overexpress, BMP2 and BMP7. WMPCs exposed to BMP4 exhibited a dose-dependent increase in GFAP⁺A2B5⁻ astrocytic differentiation after 7 div exposure to 50 ng/ml, the maximum dose tested, increased the proportion of GFAP⁺/A2B5⁻ cells from less than 1% to more than 45% (Figs 2A–C; $p < 0.001$; $F = 46.57$; by one-way ANOVA with post hoc analysis). In contrast, exogenous BMP2 and BMP7 elicited no statistically significant difference in GFAP⁺/A2B5⁻ astroglialogenesis, suggesting the selectivity of BMP4 as an astrocytic differentiation cue for adult WMPCs (see Fig 2A).

Each of the BMP ligands significantly depleted the culture of A2B5⁺GFAP⁻ progenitors with the incidence of A2B5⁺GFAP⁻ cells falling from approximately 5 to 0% at 14 days in vitro (see Figs 2D–F; $p < 0.01$; one-way ANOVA with post hoc analysis). As a corollary to the BMP-dependent depletion of A2B5⁺/GFAP⁻-defined WMPCs, each of the tested BMPs expanded the GFAP⁺A2B5⁺ pool, with BMP2, for example, achieving significance at 5ng/ml (see Figs 2D–F; $p < 0.001$; $F = 28.21$, by one-way ANOVA with post hoc analysis). These data suggest that BMP2 and BMP7 did not increase astrocytic gliogenesis per se, but rather depleted the pool of A2B5⁺GFAP⁻-defined WMPCs by driving the cells to an A2B5⁺GFAP⁺ phenotype. The latter may have represented either a transitional astroblast or type 2 astrocyte, but was antigenically distinct from the GFAP⁺A2B5⁻ glia, nominally type 1 or protoplasmic astrocytes, induced by BMP4.

Of note, both the total cell number and total live/dead cell ratios (as determined by DAPI and calcein/propidium iodide counts, respectively) remained the same among conditions; in addition, BrdU incorporation was the same in treated and untreated cultures

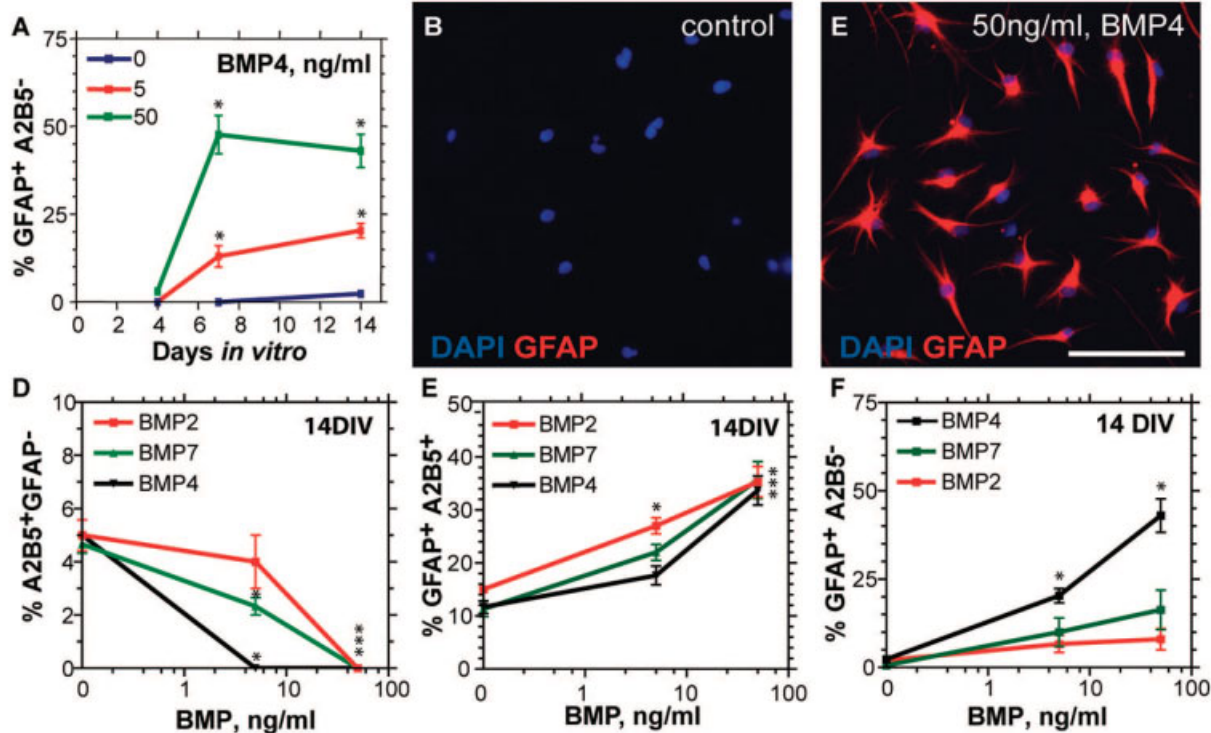


Fig 2. Bone morphogenetic protein 4 (BMP4) selectively induces astrogliogenesis. (A) Plots of the proportion of GFAP⁺A2B5⁻ identified astrocytes as a function of time after addition of either 0, 5, or 50ng/ml BMP4. (B, C) Pronounced induction of a GFAP⁺A2B5⁻ astrocytic phenotype by 50ng/ml BMP4, when assessed at 7 days in vitro (DIV). (D–F) Proportions of A2B5⁺GFAP⁻ progenitors (D), A2B5⁺GFAP⁺ transitional astroblasts or type 2 astrocytes (E), and GFAP⁺A2B5⁻ astrocytes (F), all at 14 DIV, as a function of BMP type and dose. Asterisk indicates significant difference, $p < 0.01$. GFAP = glial fibrillary acidic protein.

(data not shown). Together, these data indicate that the BMPs influenced neither the expansion nor survival of the different phenotypes assessed here, but rather directed their differentiated fate.

Noggin Maintains the WMPC Population In Vitro

To validate the role of BMP4 in inducing astrocytic differentiation by adult WMPCs, we next attempted to block glial lineage commitment by exposing the cells to noggin, a broad-spectrum BMP antagonist implicated in adult as well as developmental fate determination.^{42–45} Treatment with noggin together with 20ng/ml bFGF permitted the dose-dependent sustained maintenance of undifferentiated A2B5⁺GFAP⁻ WMPCs ($33 \pm 3.1\%$ at 14 days in vitro with 100ng/ml noggin) relative to control cultures raised in identical bFGF-supplemented serum-free media without added noggin ($9 \pm 1.4\%$; $p < 0.01$; $F = 18.36$, by ANOVA with post hoc comparisons). In addition, noggin suppressed spontaneous astrocytic differentiation (0 vs $4 \pm 0.4\%$ GFAP⁺/A2B5⁻ astrocytes at 14 days in vitro using 100ng/ml noggin; $p < 0.01$; $F = 6.05$); this occurred in a dose-dependent manner (Fig 3). Furthermore, noggin ef-

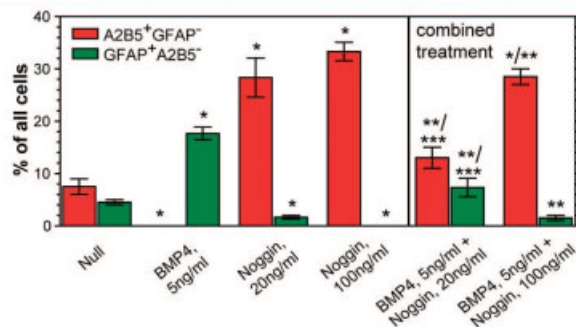


Fig 3. Noggin suppresses bone morphogenetic protein 4 (BMP4)-dependent astrogliogenesis and sustains undifferentiated white matter progenitor cells (WMPCs). This bar graph plots the relative proportions of A2B5⁺GFAP⁻ progenitors and GFAP⁺A2B5⁻ astrocytes as a function of 14 days of either BMP4 or noggin exposure, the latter at two doses. Both a significant BMP4-mediated induction of astrocyte phenotype and a noggin suppression thereof are evident. (Right) Noggin is seen to effectively block the astrocytic differentiation of WMPCs exposed to BMP4, in a noggin dose-dependent fashion. Asterisk significantly differs from null control; double asterisk differs from BMP-only treatment groups; triple asterisk differs from noggin-only groups; significance for all established as $p \leq 0.01$. GFAP = glial fibrillary acidic protein.

fectively blocked the astrocytic differentiation of WMPCs exposed to BMP4. Despite exposure to 5ng/ml BMP4, WMPC cultures coexposed to 100ng/ml noggin retained an undifferentiated progenitor population of $29 \pm 1.5\%$ at 14 days in vitro, compared with an A2B5⁺GFAP⁻ incidence of $9 \pm 1.4\%$ in cultures raised without added noggin. Administration of noggin together with 5ng/ml BMP4 was noted to suppress BMP4-induced astroglialogenesis in a noggin dose-dependent fashion ($7 \pm 3.1\%$ astrocytes in 20ng/ml noggin, relative to $1 \pm 0.6\%$ in 100ng/ml noggin; $p < 0.01$; one-way ANOVA with post hoc analysis; see Fig 3).

Discussion

In this study, we identified differences in gene expression between adult human WMPCs and the white matter environment from which they derive, so as to define those environmentally responsive signaling pathways differentially operative in these cells. By comparing the RNA profiles of adult human WMPCs with those of their parental white matter, we identified differentially expressed genes in the progenitor pool that appeared to complement others selectively

expressed by the tissue. By this means, we identified several hitherto unpredicted ligand–receptor interactions and their *cis* modifiers. Together, these data suggested: (1) the importance of the RTPZ-PTN system in WMPC self-maintenance and mobilization; (2) the potentially coregulated action of syndecan-dependent CASK release in WMPC maintenance; (3) the role of notch signaling, as reflected by the differential expression of NOTCH1, HES1, musashi, and FHL1B by sorted WMPCs, in maintaining their phenotype; (4) the role of endogenous BMP inhibitors, neuralin and BAMBI in particular, in buffering the cellular response to ambient BMPs; and (5) the likely import of PDGFRA and FGFR3 in priming these cells for differentiation. In the absence of PDGFRA and FGFR3 ligands in the ambient white matter, these patterns of quiescent gene expression might be expected to largely support the self-maintenance of WMPCs, while suppressing their differentiation.

From these data, we generated a genomics-based model for the regulatory control of adult human WMPCs, schematized in Figure 4. The following sections describe its major elements.

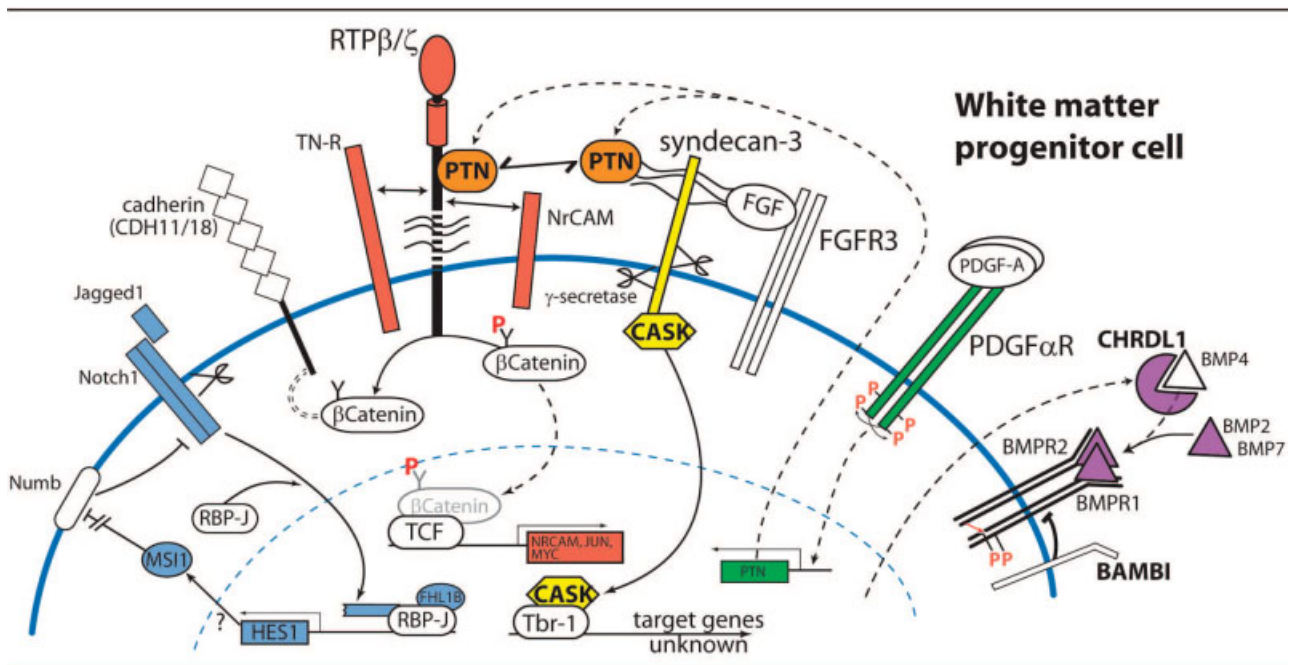


Fig 4. Signaling pathways differentially expressed by adult white matter progenitor cells (WMPCs). A total of 132 genes were differentially expressed by isolated human WMPCs relative to the white matter from which they were extracted. The assignment of these genes into coherent signaling pathways allowed us to generate this model, which may predict aspects of the metabolic regulation of WMPCs at steady state, in the adult tissue environment. The signaling pathways predominant in this model include those initiated by receptor tyrosine phosphatase- β/ζ (RTPZ), as modulated by pleiotrophin, syndecan-3, and tenascin (purple); syndecan-3 cleavage and calmodulin-activated serine kinase (CASK) translocation (yellow); notch activation (blue); PDGFRA signaling (green); and bone morphogenetic protein (BMP) signaling and inhibition thereof (purple). Genes shown in color were found to be selectively and significantly enriched in white matter progenitor cells, relative to unsorted white matter. BAMBI = BMP and activin membrane-bound inhibitor; FGF = fibroblast growth factor; FGFR3 = type 3 fibroblast growth factor receptor; PDGF = platelet-derived growth factor; PTN = pleiotrophin; TNR = tenascin-R.

Receptor Tyrosine Phosphatase- β/ζ and Its Ligands Are Abundantly and Selectively Expressed by White Matter Progenitor Cells

RTPZ was the most significantly enriched WMPC receptor gene in our analysis. Although RTPZ is expressed developmentally by radial cells and neural progenitors of the fetal ventricular zone,¹ it has also been reported to be expressed in rat oligodendrocyte progenitors.⁴⁶ Moreover, RTPZ knock-out mice exhibit impaired recovery from experimental allergic encephalitis.⁴⁷ RTPZ acts to maintain the dephosphorylated state of β -catenin,⁸ so that RTPZ-deficient WMPCs might be expected to exhibit impaired wnt signaling. In this regard, we found high levels of the secreted WNT antagonist FRZB in the WMPC pool (data not shown). FRZB has been shown to antagonize both WNT1 and WNT8 signaling.^{48,49} The deficiency in remyelination of RTPZ knock-out mice, together with the tonic expression of both RTPZ and soluble frizzled by quiescent adult human WMPCs, may suggest a role for the RTPZ-dependent dephosphorylation of β -catenin in these cells. Together, these data suggest that RTPZ signaling is required for both maintaining and mobilizing glial progenitor cells in the adult human brain.

Inhibition of Receptor Tyrosine Phosphatase- β/ζ Abrogates Progenitor Self-renewal and Induces Terminal Oligodendrocyte Differentiation

bpV(phen) is a potent oxovanadate inhibitor of tyrosine phosphatase activity.²³ We found that blockade of RTPZ using bpV(phen) abolished the undifferentiated expansion of WMPCs and promoted their oligodendrocytic differentiation. However, because known pharmacological inhibitors of RTPZ suppress all receptor tyrosine phosphatases, we could not be confident of the molecular specificity of this effect, notwithstanding the high differential expression of RTPZ by WMPCs. To definitively ascertain the import of RTPZ in phosphatase inhibition-induced differentiation, we thus developed a lentiviral shRNAi knock-down vector specific for the long receptor isoform of RTPZ. Infection of WMPCs with the lentiviral RTPZ shRNAi replicated the results obtained with bpV(phen), in that GFP⁺ transductants differentiated largely as oligodendrocytes and exhibited a significant reduction in the A2B5⁺ progenitor pool.

Pleiotrophin Expression May Act as an Autocrine Modulator of Receptor Tyrosine Phosphatase- β/ζ Activity

PTN inhibits RTPZ-dependent dephosphorylation of β -catenin, and by so doing may serve to modulate wnt signaling.⁸ In addition to the strong differential expression of PTN, our microarray analyses also showed a number of other *cis* heterophilic ligands of RTPZ,

such as NrCAM and the CSPGs, the expression of which may serve to further modulate the phosphatase activity of RTPZ. This pattern of gene expression suggests that parallel pathways may operate to dynamically regulate wnt signaling in adult WMPCs. Because wnt signaling can actively drive neural progenitor expansion,⁵⁰ the reversible suppression of this pathway may be required for the maintenance of progenitors in a quiescent though mitotically competent state.

Syndecan and Calmodulin-Activated Serine Kinase-Dependent Signaling Comprise a Parallel Regulatory Pathway

Our model accommodates the expression of syndecan-3 and its known binding partners, a number of which, including CASK, FGFR3, and PTN, were differentially expressed by adult WMPCs. Although syndecan-3 has been shown to act as a coreceptor for both PTN and FGF2, syndecan-3 can also transduce extracellular signals via ligand-induced, γ -secretase-mediated proteolytic cleavage of its C-terminal C2 domain.²⁴ In particular, release of the C-terminal domain frees the syndecan-3 bound protein calcium/CASK to translocate to the nucleus, where it can act as a transcriptional activator through the T-box transcription factor TBR1, a brachyury family member²⁵ that was indeed present in the sorted WMPCs. Although the downstream targets of TBR1 and its family members are largely unknown, its induction may thus be involved in regulating the fate of adult WMPCs.

Constitutive Activation of Notch Pathway

The adult human WMPC resembles the rodent oligodendrocyte progenitor with regard to the notch signaling pathway.³⁶ WMPCs express high levels of both the notch receptor, NOTCH1, and its downstream effectors HES1 and musashi1. Indeed, the novel LIM-domain-containing protein FHL1B, which appears to act downstream of notch to bind and transcriptionally activate RBP-J, was substantially enriched in WMPCs. Although the precise function of FHL1B in oligoneogenesis is unknown, it is worth noting that the developmental expression pattern of this gene clusters with that of the oligodendrocyte lineage markers PDGF α R, olig1, and olig2 during human fetal ventricular zone development (unpublished data). Furthermore, FHL1 expression has been described in microarray studies on skin, neural, hematopoietic, and embryonic stem cell populations, suggesting a more widespread role of FHL1 in diverse stem and progenitor cell populations.^{51,52} Surprisingly, the notch ligand JAG1 was also differentially expressed by adult WMPCs. During development, oligodendrocyte progenitors do not appear to express jagged.³⁶ However, its expression by adult WMPCs may suggest a degree of lateral activation of notch signaling that may serve to maintain contiguous

progenitors in an undifferentiated state pending mobilization.⁵³

Notch signaling typically results in the upregulation of HES1, which itself serves as a negative regulator of differentiation, as manifested by its repression of MASH1 and OLIG2 transcription. As a result, it was surprising to note the coexpression of MASH1 and HES1 by adult human WMPCs. Yet, although our data suggest that MASH1 and HES1 are coexpressed by single cells, it might also be the case that the WMPC population contains multiple stages of parenchymal progenitor ontogeny.

The Bone Morphogenetic Proteins and Their Antagonists

BMP ligands can promote the differentiation of neural progenitor cells toward an astrocytic fate, and can inhibit both neurogenesis and oligodendroglial differentiation.⁵⁴ We have shown that when raised at low density and high purity, in the absence of either autocrine or paracrine growth factors, adult human WMPCs exhibit a pronounced neurogenic capacity and are able to differentiate into functional neurons both in vitro and, on transplantation, in vivo.² In this study, we have shown that WMPCs express significantly more BMP2 and BMP7 than the surrounding white matter, while expressing both membrane-bound (BAMBI) and soluble (neuralin) inhibitors of other BMPs. Exposure to BMP4 resulted in a strong dose-dependent increase in GFAP-defined astroglialogenesis and a corresponding depletion of A2B5-defined WMPCs. Conversely, neither BMP2 nor BMP7 exposure increased astroglialogenesis, though high levels of each were associated with a relative depletion of WMPCs. Treatment with the broad-spectrum BMP antagonist noggin then permitted the sustained maintenance of undifferentiated WMPCs, and significantly suppressed BMP-induced astrocytic differentiation. These results support a model of autocrine maintenance of WMPCs by BMP2- and BMP7-regulated pathways, with a concurrent tonic inhibition of BMP4, the activity of which would otherwise serve as a strong stimulus to astrocytic production.

Tyrosine Kinase Receptors

Adult human WMPCs, like rat oligodendrocyte progenitors, respond to bFGF as a mitogen and suppress terminal differentiation.¹ Our data indicate that WMPCs express high levels of the FGFR3, which might thereby constitute an important target for manipulating WMPC proliferation in vitro and in vivo. Of the three identified endogenous ligands of FGFR3, FGF1 (acidic), FGF4, and FGF9, we detected expression of FGF1 and FGF9 in our microarrays. Although both FGF1 and FGF9 have been shown to be mitogenic for A2B5⁺ glial progenitors,^{55,56} only FGF1 was significantly greater in the white matter dissociate than

in the sorted WMPCs. Like FGFR3, the PDGFRA was also highly expressed by WMPCs. PDGF is a mitogen for rodent and human glial progenitors and can initiate oligodendrocytic differentiation. Moreover, PDGF signaling has been shown to induce PTN mRNA expression in 3T3 cells.⁵⁷ Together, these results suggest a scheme whereby PDGFRA signaling may induce PTN, followed by the PTN-mediated coregulation of RTPZ and syndecan/CASK-triggered pathways (see Fig 4).

Influences of the Epileptic Environment

In this study, our genomics analysis was done on RNA extracted from white matter derived from patients with medication-refractory epilepsies. Although we have previously found that epileptic and nonepileptic white matter share abundant populations of WMPCs with multilineage capacity,² and that WMPCs derived from both sources behave identically in vitro under a variety of growth conditions, it cannot be assumed that the gene expression patterns of the two are homologous. To the contrary, the epileptic environment may exert specific effects on resident WMPCs that can potentially manifest in their expression profiles. In part to minimize the effect of any such environmental bias, we normalized the expression profile of each sorted progenitor cell isolate against that of the dissociated but unsorted white matter from which it derived. This normalization step served to select those genes differentially expressed by WMPCs, relative to the tissue from which they derived. As a result, any genes whose expression might have been altered in epilepsy should have been filtered out of our list of genes differentially expressed by WMPCs. That being said, any genes induced by the epileptic environment specifically in WMPCs, which were not similarly activated in local astrocytes or other parenchymal phenotypes, might have been identified by our analysis as differentially expressed by WMPCs. Thus, although the epileptic environment of these cells might have influenced their gene expression patterns, the nature of our analysis would have only detected such effects on genes already differentially expressed by WMPCs. Future comparisons of WMPCs derived from normal and epileptic brains will be needed to establish the effects of the epileptic environment on the self-renewal and fate of adult WMPCs.

Overview

We have analyzed the differentially expressed transcripts of a highly enriched progenitor cell population isolated from the adult brain, and assessed those transcripts in the context of complementary patterns of gene expression in the and local matter. On that basis, we have established a model for the pathways and interactions thereof by which glial progenitor cells are

regulated in the adult human white matter, and by which oligodendrocytic differentiation may be determined. At baseline, these interactions would appear to support the self-maintenance and turnover of WMPCs, while suppressing their directed differentiation. As the model of Figure 4 illustrates, these pathways enjoy substantial cross talk, that might permit the system to respond readily to environmental change, while buffering it from perturbation by any single molecular stimulus. As such, these pathways may be targeted at a number of loci, for both genetic and pharmacological modulation of progenitor cell turnover and fate.

This work was supported by the NIH (National Institute of Neurological Disorders and Stroke, R01NS039559), the National Multiple Sclerosis Society, Aventis Pharmaceuticals, Berlex Bioscience, and the German Academic Exchange Service (DAAD; B.W.).

References

- Roy NS, Wang S, Harrison-Restelli C, et al. Identification, isolation, and promoter-defined separation of mitotic oligodendrocyte progenitor cells from the adult human subcortical white matter. *J Neurosci* 1999;19:9986–9995.
- Nunes MC, Roy NS, Keyoung HM, et al. Identification and isolation of multipotential neural progenitor cells from the subcortical white matter of the adult human brain. *Nat Med* 2003;9:439–447.
- Windrem MS, Roy NS, Wang J, et al. Progenitor cells derived from the adult human subcortical white matter disperse and differentiate as oligodendrocytes within demyelinated lesions of the rat brain. *J Neurosci Res* 2002;69:966–975.
- Milliken G, Johnson DK. *Analysis of messy data*. Vol. 1. Belmont, CA: Wadsworth, 1984.
- Benjamini Y, Hochberg Y. Controlling the false discovery rate: a practical and powerful approach to multiple testing. *J R Stat Soc* 1995;57:289–300.
- Yuan B, Latek R, Hossbach M, et al. siRNA Selection Server: an automated siRNA oligonucleotide prediction server. *Nucleic Acids Res* 2004;32:W130–W134.
- Rubinson DA, Dillon CP, Kwiatkowski AV, et al. A lentivirus-based system to functionally silence genes in primary mammalian cells, stem cells and transgenic mice by RNA interference. *Nat Genet* 2003;33:401–406.
- Meng K, Rodriguez-Pena A, Dimitrov T, et al. Pleiotrophin signals increased tyrosine phosphorylation of beta-catenin through inactivation of the intrinsic catalytic activity of the receptor-type protein tyrosine phosphatase beta/zeta. *Proc Natl Acad Sci USA* 2000;97:2603–2608.
- Eisenbarth GS, Walsh FS, Nirenberg M. Monoclonal antibody to a plasma membrane antigen of neurons. *Proc Natl Acad Sci U S A* 1979;76:4913–4917.
- Raff MC, Miller RH, Noble M. A glial progenitor cell that develops in vitro into an astrocyte or an oligodendrocyte depending on culture medium. *Nature* 1983;303:390–396.
- Farrer RG, Quarles RH. GT3 and its O-acetylated derivative are the principal A2B5-reactive gangliosides in cultured O2A lineage cells and are down-regulated along with O-acetyl GD3 during differentiation to oligodendrocytes. *J Neurosci Res* 1999;57:371–380.
- Fancy SP, Zhao C, Franklin RJ. Increased expression of Nkx2.2 and Olig2 identifies reactive oligodendrocyte progenitor cells responding to demyelination in the adult CNS. *Mol Cell Neurosci* 2004;27:247–254.
- Lu QR, Yuk D, Alberta JA, et al. Sonic hedgehog-regulated oligodendrocyte lineage genes encoding bHLH proteins in the mammalian central nervous system. *Neuron* 2000;25:317–329.
- Watanabe M, Hadzic T, Nishiyama A. Transient upregulation of Nkx2.2 expression in oligodendrocyte lineage cells during remyelination. *GLIA* 2004;46:311–322.
- Curtis R, Hardy R, Reynolds R, et al. Down-regulation of GAP-43 during oligodendrocyte development and lack of expression by astrocytes in vivo: implications for macroglial differentiation. *Eur J Neurosci* 1991;3:876–886.
- Hosack DA, Dennis G Jr, Sherman BT, et al. Identifying biological themes within lists of genes with EASE. *Genome Biol* 2003;4:R70.
- Mosselman S, Claesson-Welsh L, Kamphuis JS, Van Zoelen EJ. Developmentally regulated expression of two novel platelet-derived growth factor alpha-receptor transcripts in human teratocarcinoma cells. *Cancer Res* 1994;54:220–225.
- Sussman CR, Vartanian T, Miller RH. The ErbB4 neuregulin receptor mediates suppression of oligodendrocyte maturation. *J Neurosci* 2005;25:5757–5762.
- Canoll PD, Musacchio JM, Hardy R, et al. GGF/neuregulin is a neuronal signal that promotes the proliferation and survival and inhibits the differentiation of oligodendrocyte progenitors. *Neuron* 1996;17:229–243.
- Bansal R, Pfeiffer SE. FGF-2 converts mature oligodendrocytes to a novel phenotype. *J Neurosci Res* 1997;50:215–228.
- Molina-Holgado E, Vela JM, Arevalo-Martin A, et al. Cannabinoids promote oligodendrocyte progenitor survival: involvement of cannabinoid receptors and phosphatidylinositol-3 kinase/Akt signaling. *J Neurosci* 2002;22:9742–9753.
- Winkler S, Stahl RC, Carey DJ, Bansal R. Syndecan-3 and perlecan are differentially expressed by progenitors and mature oligodendrocytes and accumulate in the extracellular matrix. *J Neurosci Res* 2002;69:477–487.
- Posner BI, Faure R, Burgess JW, et al. Peroxovanadium compounds. A new class of potent phosphotyrosine phosphatase inhibitors which are insulin mimetics. *J Biol Chem* 1994;269:4596–4604.
- Schulz JG, Annaert W, Vandekerckhove J, et al. Syndecan 3 intramembrane proteolysis is presenilin/gamma-secretase-dependent and modulates cytosolic signaling. *J Biol Chem* 2003;278:48561–48567.
- Hsueh YP, Wang TF, Yang FC, Sheng M. Nuclear translocation and transcription regulation by the membrane-associated guanylate kinase CASK/LIN-2. *Nature* 2000;404:298–302.
- Milev P, Chiba A, Haring M, et al. High affinity binding and overlapping localization of neurocan and phosphacan/protein-tyrosine phosphatase-zeta/beta with tenascin-R, amphoterin, and the heparin-binding growth-associated molecule. *J Biol Chem* 1998;273:6998–7005.
- Sakurai T, Lustig M, Nativ M, et al. Induction of neurite outgrowth through contactin and Nr-CAM by extracellular regions of glial receptor tyrosine phosphatase beta. *J Cell Biol* 1997;136:907–918.
- Milev P, Friedlander DR, Sakurai T, et al. Interactions of the chondroitin sulfate proteoglycan phosphacan, the extracellular domain of a receptor-type protein tyrosine phosphatase, with neurons, glia, and neural cell adhesion molecules. *J Cell Biol* 1994;127:1703–1715.
- Hillenbrand R, Molthagen M, Montag D, Schachner M. The close homologue of the neural adhesion molecule L1 (CHL1): patterns of expression and promotion of neurite outgrowth by heterophilic interactions. *Eur J Neurosci* 1999;11:813–826.
- Goldman SA, Williams S, Barami K, et al. Transient coupling of Ng-CAM expression to NgCAM-dependent calcium signaling during migration of new neurons in the adult songbird brain. *Mol Cell Neurosci* 1996;7:29–45.

31. Von Bohlen Und Halbach F, Taylor J, Schachner M. Cell type-specific effects of the neural adhesion molecules L1 and N-CAM on diverse second messenger systems. *Eur J Neurosci* 1992;4:896–909.
32. Pesheva P, Gloor S, Schachner M, Probstmeier R. Tenascin-R is an intrinsic autocrine factor for oligodendrocyte differentiation and promotes cell adhesion by a sulfatide-mediated mechanism. *J Neurosci* 1997;17:4642–4651.
33. Weber P, Bartsch U, Rasband MN, et al. Mice deficient for tenascin-R display alterations of the extracellular matrix and decreased axonal conduction velocities in the CNS. *J Neurosci* 1999;19:4245–4262.
34. Asher RA, Morgenstern DA, Shearer MC, et al. Versican is up-regulated in CNS injury and is a product of oligodendrocyte lineage cells. *J Neurosci* 2002;22:2225–2236.
35. Chen ZJ, Ughrin Y, Levine JM. Inhibition of axon growth by oligodendrocyte precursor cells. *Mol Cell Neurosci* 2002;20:125–139.
36. Wang S, Sdrulla AD, DiSibio G, et al. Notch receptor activation inhibits oligodendrocyte differentiation. *Neuron* 1998;21:63–75.
37. Lee SM, Li HY, Ng EK, et al. Characterization of a brain-specific nuclear LIM domain protein (FHL1B) which is an alternatively spliced variant of FHL1. *Gene* 1999;237:253–263.
38. Imai T, Tokunaga A, Yoshida T, et al. The neural RNA-binding protein Musashi1 translationally regulates mammalian numb gene expression by interacting with its mRNA. *Mol Cell Biol* 2001;21:3888–3900.
39. Gaiano N, Nye JS, Fishell G. Radial glial identity is promoted by Notch1 signaling in the murine forebrain. *Neuron* 2000;26:395–404.
40. Sakuta H, Suzuki R, Takahashi H, et al. Ventroptin: a BMP-4 antagonist expressed in a double-gradient pattern in the retina. *Science* 2001;293:111–115.
41. Onichtchouk D, Chen YG, Dosch R, et al. Silencing of TGF-beta signalling by the pseudoreceptor BAMBI. *Nature* 1999;401:480–485.
42. Chmielnicki E, Benraiss A, Economides AN, Goldman SA. Adenovirally expressed noggin and brain-derived neurotrophic factor cooperate to induce new medium spiny neurons from resident progenitor cells in the adult striatal ventricular zone. *J Neurosci* 2004;24:2133–2142.
43. Kondo T, Raff MC. A role for Noggin in the development of oligodendrocyte precursor cells. *Dev Biol* 2004;267:242–251.
44. Lim DA, Tramontin AD, Trevejo JM, et al. Noggin antagonizes BMP signaling to create a niche for adult neurogenesis. *Neuron* 2000;28:713–726.
45. Zimmerman LB, Jesus-Escobar JM, Harland RM. The Spemann organizer signal noggin binds and inactivates bone morphogenetic protein 4. *Cell* 1996;86:599–606.
46. Canoll PD, Petanceska S, Schlessinger J, Musacchio JM. Three forms of RPTP-beta are differentially expressed during gliogenesis in the developing rat brain and during glial cell differentiation in culture. *J Neurosci Res* 1996;44:199–215.
47. Harroch S, Furtado GC, Brueck W, et al. A critical role for the protein tyrosine phosphatase receptor type Z in functional recovery from demyelinating lesions. *Nat Genet* 2002;32:411–414.
48. Wang S, Krinks M, Lin K, et al. Frzb, a secreted protein expressed in the Spemann organizer, binds and inhibits Wnt-8. *Cell* 1997;88:757–766.
49. Leyns L, Bouwmeester T, Kim SH, et al. Frzb-1 is a secreted antagonist of Wnt signaling expressed in the Spemann organizer. *Cell* 1997;88:747–756.
50. Zechner D, Fujita Y, Hulsken J, et al. beta-Catenin signals regulate cell growth and the balance between progenitor cell expansion and differentiation in the nervous system. *Dev Biol* 2003;258:406–418.
51. Ramalho-Santos M, Yoon S, Matsuzaki Y, et al. “Stemness”: transcriptional profiling of embryonic and adult stem cells. *Science* 2002;298:597–600.
52. Tumber T, Guasch G, Greco V, et al. Defining the epithelial stem cell niche in skin. *Science* 2004;303:359–363.
53. John GR, Shankar SL, Shafiq-Zagardo B, et al. Multiple sclerosis: re-expression of a developmental pathway that restricts oligodendrocyte maturation. *Nat Med* 2002;8:1115–1121.
54. Gross RE, Mehler MF, Mabie PC, et al. Bone morphogenetic proteins promote astroglial lineage commitment by mammalian subventricular zone progenitor cells. *Neuron* 1996;17:595–606.
55. Naruo K, Seko C, Kuroshima K, et al. Novel secretory heparin-binding factors from human glioma cells (glia-activating factors) involved in glial cell growth. Purification and biological properties. *J Biol Chem* 1993;268:2857–2864.
56. Engele J, Bohn MC. Effects of acidic and basic fibroblast growth factors (aFGF, bFGF) on glial precursor cell proliferation: age dependency and brain region specificity. *Dev Biol* 1992;152:363–372.
57. Li YS, Gurrieri M, Deuel TF. Pleiotrophin gene expression is highly restricted and is regulated by platelet-derived growth factor. *Biochem Biophys Res Commun* 1992;184:427–432.
58. Richter-Landsberg C, Gorath M. Developmental regulation of alternatively spliced isoforms of mRNA encoding MAP2 and tau in rat brain oligodendrocytes during culture maturation. *J Neurosci Res* 1999;56:259–270.
59. Canoll PD, Barnea G, Levy JB et al. The expression of a novel receptor-type tyrosine phosphatase suggests a role in morphogenesis and plasticity of the nervous system. *Brain Res. Dev. Brain Res.* 1993;75:293–298.